# Long-range many-body polyelectrolyte bridging interactions

Rudi Podgornik[a)]
*Department of Physics, University of Ljubljana, Jadranska 19, 1000 Ljubljana, Slovenia, Department of Theoretical Physics, J. Stefan Institute, Janova 39, SI-1000 Ljubljana, Slovenia, and Laboratory of Physical and Structural Biology, National Institute of Child Health and Human Development (NICHD), Building 9 Room 1E116, National Institutes of Health, Bethesda Maryland 20892-0924*

Wayne M. Saslow
*Department of Physics, Texas A&M University, College Station, Texas 77840-4242 and Laboratory of Physical and Structural Biology, National Institute of Child Health and Human Development (NICHD), Building 9 Room 1E116, National Institutes of Health, Bethesda, Maryland 20892-0924*

(Received 26 January 2005; accepted 21 March 2005; published online 24 May 2005)

We investigate polyelectrolyte bridging interactions mediated by charged, flexible, polyelectrolyte chains between fixed cylindrical macroions of opposite charge in a two-dimensional hexagonal crystalline array. We show that in the asymptotic regime of small macroion density, the polyelectrolyte-mediated attraction is long range, falling off approximately linearly with the macroion array density. We investigate the polyelectrolyte free energy as a function of the macroion density and derive several analytic limiting laws valid in different regimes of the parameter space. © *2005 American Institute of Physics*. [DOI: 10.1063/1.1908870]

## I. INTRODUCTION

Charged polymers are ubiquitous in colloidal systems and soft matter in general,[1,2] and play a fundamental role in determining the interactions between, as well as the stability and structure of, various (macro)molecular assemblies. Charged polymers are sufficiently different to set them apart from noncharged polymers.[3] Their effect on colloidal interactions has been studied and exploited in various technological contexts ranging from the paper industry to the pharmaceutical industry.[4] Their most basic role nevertheless is played in the biological context. They are essential and fundamental components of the cellular environment and make their mark in its every structural and functional aspects.[5] It is thus no surprise that the behavior of charged polymer chains in the biological context has been one of the major foci of soft matter research.[6]

The connectivity between charged segments along the polymer chain is an essential feature of polyelectrolytes and can often lead to a very peculiar interaction, whereby long-charged polymers can mediate interactions between macroions of opposite charge (for recent reviews see Refs. 7 and 8). The term bridging interactions is usually applied to this situation, where a single chain can adsorb to two (or more) oppositely charged macroions and via its connectivity mediate attractive interactions between them. These interactions have been studied intensively both experimentally as well as theoretically.

Polyelectrolyte chains in the bulk, worked out at different levels of approximation,[8] are reasonably well understood. Confined (neutral) polymers are also well understood, and the forces between confining surfaces have been studied at various levels of approximation.[9] The two were first brought together, i.e., charged interfaces with charged polymers, in the seminal work of Muthukumar.[10] A major conclusion of this work was that, due to the connectivity of the polyelectrolyte chain, its behavior bears almost no resemblance to the case of confined unconnected ions. A self-consistent field theory, akin to the usual Poisson–Boltzmann theory of electrostatic interactions in colloidal systems, has been proposed for confined polyelectrolytes and applied successfully to polyelectrolyte-mediated interactions between charged surfaces.[11] This approach was later generalized to include steric interactions between polymer segments on adsorption and polyelectrolyte-mediated interaction.[12,13] For small macroions with free[14] or grafted polyelectrolyte chains a different approach was found to be more convenient, based on a quadratic variational ansatz.[15] It allows for an elegant and straightforward evaluation of the polyelectrolyte-mediated interactions in the geometry where self-consistent field theory would be more difficult to solve.

All of the above approaches are, however, based on a two-body approximation. The polyelectrolyte bridging is assumed to involve at most two macroions, be they macromolecular surfaces or indeed whole macromolecules. Recent experiments on DNA-polycation complexes,[16] however, suggest that polyelectrolyte bridging might involve many particles as well. A single polyelectrolyte chain can bridge several macroions conferring an interaction that cannot be approximated on a pairwise level. We take this picture as a motivation for our present work, which investigates the many-body bridging interactions that occur when a single polyelectrolyte chain mediates interactions between several oppositely charged macroions. The theoretical framework for this analysis is based on the Edwards model of a flexible chain[17] in an external-screened Coulomb potential provided by the lattice of charged macroions. In what follows we will concentrate exclusively on conceptual framework and will

[a)]Electronic mail: rudi@helix.nih.gov

 

try to derive approximate limiting laws for the polyelectrolyte-mediated interactions. We will leave detailed numerical solutions to a forthcoming paper.

The present work is, apart from the difference in geometry, closely related to previous work of one of the authors.[11] There, in a background ionic solution, charged polymers (e.g., of positive sign) produced a short-range attraction between two charged planes (e.g., of negative sign). Assuming no lateral inhomogeneities, the problem discussed was effectively one dimensional (1D). Here for a two-dimensional (2D) hexagonal lattice model in a background ionic solution, charged polymers (e.g., positively charged polylysine or polyarginine of between 30 and 100 monomers) produce a long-range attraction in an array of rodlike cylindrical macroions (e.g., negatively charged DNA molecules). We show that this long-range attraction stems from bridging configurations of flexible polyelectrolyte chains in the macromolecular array at sufficiently low macromolecular densities. This attraction might add or compete with the polycation correlation effect.[16,18]

The outline of the paper is as follows. We first formulate the model of charged polyelectrolyte chains and apply it on the mean-field level to a periodic hexagonal lattice of oppositely charged cylindrical rods. In order to make this problem transparent and simply solvable we first assume that the strength of the macroion-polyelectrolyte interaction is constant. We then remove this constraint in the Wigner–Seitz calculation. The eigenvalue equation in the lattice model is directly analogous to that for electrons in a 2D crystal. We calculate the eigenenergy for a few of the lowest-lying eigenstates using a reciprocal lattice vector (RLV) basis set, and we show that for sufficiently strongly charged macroions it leads to attractive polyelectrolyte-mediated interactions that correspond to polyelectrolyte bridging configurations. The slow convergence of the RLV formulation together with the assumption of fixed, i.e., macroion density-independent strength of the interaction, precludes us from establishing any firm limiting laws. In order to get stronger analytical estimates and/or limiting laws we then formulate the same problem on the Wigner–Seitz cell level and solve it approximately with the Wentzel–Kramers–Brillouin (WKB) ansatz. This allows us both to numerically estimate the critical linear charge density of the macroions that leads to attractive bridging interactions and to obtain the form of bridging interaction as a function of the macroion density. We conclude the paper with a discussion of the significance of these findings as well as with a proposal for more detailed numerical calculations of the interaction for the full range of macromolecular densities.

## II. MODEL OF A CHARGED ASSEMBLY OF STIFF RODS AND FLEXIBLE POLYELECTROLYTES

The model system has two components, in addition to the background ionic solution. The first component is a set of infinitely stiff, charged, cylindrical macroions (e.g., DNA) of radius $a$ on a 2D hexagonal lattice with lattice constant $R$. Each macroion acts as a source of screened Debye–Hückel electrostatic potential.[19] The second component is a set of oppositely charged flexible polyelectrolyte chains (e.g., positively-charged polyelectrolyte chains). We assume that the most important part of the total energy is the interaction of the flexible chains with fixed macroion charges and disregard self-interactions among the polyelectrolyte chains. The latter would in fact only renormalize the persistence length, an effect which we will disregard. Moreover, we also neglect the interaction of flexible chains with one another, an approximation valid for sufficiently low polyelectrolyte density. A schematic representation of the geometry and the model is given in Fig. 1.

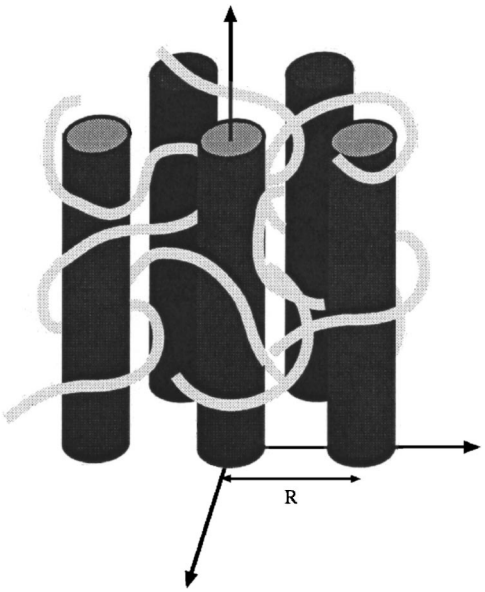


FIG. 1. A schematic presentation of the model system. Long infinitely stiff charged macroions of radius $a$ occupy the sites of a 2D hexagonal array with lattice spacing $R$. Oppositely charged flexible polyelectrolyte chains interact with an electrostatic field provided by the lattice of macroions.

The polyelectrolyte chains are described with a continuum Edwards model[17] of $N$ freely jointed segments, each of Kuhn's length, $\ell$, with a total contour length $N\ell$. The total number of polymer chains is $\mathcal{N}$. The total number of macroions is taken as $\mathcal{M}$. As indicated, all electrostatic interactions are mediated by screened Debye–Hückel interactions.[8] The configurational part of the Hamiltonian of a single chain can be written as[17]

$$\beta\mathcal{H}[\mathbf{r}(n)] = \frac{3}{2\ell^2}\int_0^N \left[\frac{d\mathbf{r}(n)}{dn}\right]^2 dn + \beta\int_0^N V[\mathbf{r}(n)]dn, \quad (1)$$

where $\beta=(k_BT)^{-1}$ is the inverse thermal energy and $\mathbf{r}(n)$ is the position of the $n$th segment of the polyelectrolyte chain. Since by assumption the chains do not interact with one another but interact only with the macroions, the total Hamiltonian decouples into a sum of one-particle Hamiltonians. The many-chain effects thus show up additively in the free energy, where the result for the single chain is simply multiplied by the total number of chains $\mathcal{N}$ (see below).

The external interaction potential of fixed macroions is characterized by the potential energy $V[\mathbf{r}(n)]$, which represents the screened electrostatic interaction between one of the flexible polyelectrolyte segments and all of the charge on the macroions. Taking the (negative) charge per unit length

along the macroion rods to be $-\mu$ and the charge per segment of the flexible polyelectrolyte to be $e$, we have

$$V(\boldsymbol{\rho}) = -\frac{\mu e}{4\pi\epsilon\epsilon_0}\int_{-\infty}^{+\infty}\frac{e^{-\kappa|\mathbf{r}-\mathbf{r}'|}}{|\mathbf{r}-\mathbf{r}'|}dz$$
$$= -\frac{\mu e}{4\pi\epsilon\epsilon_0}K_0(\kappa\rho) = -k_BTw_0K_0(\kappa\rho), \tag{2}$$

where the long axis of the macromolecules is oriented along the $z$ axis. Here $K_0(x)$ is the cylindrical Bessel function, $\rho=|\rho|$, with $\rho=(x,y)$, and the dimensionless interaction strength $w_0 \equiv \mu e/(4\pi\epsilon\epsilon_0 k_BT) = (\mu/e_0)(e/e_v)\ell_B$, where $\ell_B$ is the standard Bjerrum length. We assume that the macroion radius $a$ is small and that their finite size, which can be effectively hidden in $w_0$, can be neglected. The total interaction potential, obtained by summing the above expression over all the 2D hexagonal lattice sites, is then

$$V(\boldsymbol{\rho}) = -k_BTw_0\sum_i K_0(|\boldsymbol{\rho}-\boldsymbol{\rho}_i|). \tag{3}$$

Clearly the interaction between a polyelectrolyte chain and the macroions depends only on the $(x,y)$ coordinates since the system is assumed homogeneous in the $z$ direction, i.e., its properties do not depend on the $z$ coordinate. For DNA this is a reasonable assumption only for low densities.[20] Furthermore the interaction potential has the same symmetry as the underlying lattice of charged macroions.

For the Hamiltonian Eq. (1), and for a system that is homogeneous in the $z$ direction, the Green function of the polyelectrolyte chain, being the probability density that the chain of $N$ links will end up at $\boldsymbol{\rho}'$ if it starts from $\boldsymbol{\rho}$, is defined by[21]

$$\mathcal{G}(\boldsymbol{\rho},\boldsymbol{\rho}';N) = \int_{\boldsymbol{\rho}(0)=\boldsymbol{\rho}'}^{\boldsymbol{\rho}(N)=\boldsymbol{\rho}}\mathcal{D}[\boldsymbol{\rho}(n)]$$
$$\times\exp\left\{-\frac{3}{2\ell^2}\int_0^N\left[\frac{d\boldsymbol{\rho}(n)}{dn}\right]^2 dn\right.$$
$$\left.-\beta\int_0^N V[\boldsymbol{\rho}(n)]dn\right\}, \tag{4}$$

From the Green function it is straightforward to obtain the corresponding free energy of the chain in the form[21]

$$\mathcal{F} = -k_BT\log\left[\int\int\mathcal{G}(\boldsymbol{\rho},\boldsymbol{\rho}';N)d^2\boldsymbol{\rho}d^2\boldsymbol{\rho}'\right]. \tag{5}$$

The definition of the Green function for a system homogeneous in the $z$ direction leads in a straightforward way to the solution of a "Schrödinger equation" of the form[21]

$$\frac{\partial\mathcal{G}(\boldsymbol{\rho},\boldsymbol{\rho}',N)}{\partial N} - \frac{\ell^2}{6}\nabla_\perp^2\mathcal{G}(\boldsymbol{\rho},\boldsymbol{\rho}',N) + \beta V(\boldsymbol{\rho})\mathcal{G}(\boldsymbol{\rho},\boldsymbol{\rho}',N)$$
$$= \delta^2(\boldsymbol{\rho}-\boldsymbol{\rho}')\,\delta(N), \tag{6}$$

where $\nabla_\perp^2$ is the 2D Laplace operator in the $(x,y)$ plane. If we now introduce the standard eigenfunction expansion for the Green function

$$\mathcal{G}(\boldsymbol{\rho},\boldsymbol{\rho}',N) = \sum_n \psi_n(\boldsymbol{\rho})\psi_n(\boldsymbol{\rho}')e^{-E_nN} \tag{7}$$

we obtain the Schrödinger equation for the eigenfunction $\psi_n(\boldsymbol{\rho})$ and their dimensionless eigenvalues $E_n$ in the form

$$\left(-\frac{\ell^2}{6}\nabla_\perp^2 - w_0\sum_i K_0(|\boldsymbol{\rho}-\boldsymbol{\rho}_i|)\right)\psi_n(\boldsymbol{\rho}) = E_n\psi_n(\boldsymbol{\rho}), \tag{8}$$

where we employed Eq. (3). The eigenfunctions, being real, are subject to normalization $\int\psi_n^2 d^2\boldsymbol{\rho}=1$. The above equation is very similar to the Schrödinger equation for an electron in a 2D lattice[22] except that the unscreened Coulomb interaction is replaced by the screened Debye–Hückel interaction. In what follows we shall exploit this obvious analogy.

Since in Eq. (7) the exponent depends linearly on the length of the chain $N$, for a sufficiently long chain only the lowest eigenvalue and thus only the lowest term in the sum Eq. (7) should matter. This statement is usually known as the *ground-state dominance* ansatz in the polymer literature.[23] In this limit the Green function and the polyelectrolyte free energy assume the approximate forms

$$\mathcal{G}(\boldsymbol{\rho},\boldsymbol{\rho}',N) \cong \psi_0(\boldsymbol{\rho})\psi_0(\boldsymbol{\rho}')e^{-E_0N}$$

and

$$\mathcal{F} \cong k_BTE_0N, \tag{9}$$

whereas the monomer density can be written as

$$\rho(\boldsymbol{\rho}) \cong \psi^2(\boldsymbol{\rho}). \tag{10}$$

One should differentiate here between the above density and the 2D radius vector $\boldsymbol{\rho}=(x,y)$. The lowest-lying eigenvalue of the Schrödinger equation thus determines the polyelectrolyte free energy directly. Similarly the square of the eigenfunction determines the polyelectrolyte density in complete analogy with quantum mechanics. This simple correspondence is somewhat obscured if one goes beyond the ground-state dominance ansatz. In order to get the complete free energy one has to multiply the above result by the number of the chains, thus

$$\mathcal{F} \cong k_BTE_0(N\mathcal{N}) = k_BTE_0\mathbb{N}, \tag{11}$$

where $\mathbb{N}$ is now the total number of monomers in the system. The additivity of the free energy applies only on the level where the interchain interactions can be neglected.

## III. PERIODIC LATTICE OF RODS

We now consider the Schrödinger equation [Eq. (8)] explicitly. For finite-size impenetrable macroions the boundary condition at their surface is that the polyelectrolyte density is zero, or $\rho(|\boldsymbol{\rho}|=a)=\psi^2(|\boldsymbol{\rho}|=a)=0$. Therefore, at the surface of the macroion $\psi(|\boldsymbol{\rho}|=a)=0$, where $\psi$ is now the eigenfunction corresponding to the lowest-energy eigenvalue. For simplicity, we treat each rod as having zero radius, so the boundary condition $\psi(|\boldsymbol{\rho}|=0)=0$ applies on the axis of each rod. Near each rod the potential $V(\boldsymbol{\rho})$ is strongly attractive (i.e., negative), and dominates the eigenenergy $E_n$. Hence, near the rod the curvature of the wave function is negative, corresponding

to an oscillatory behavior; starting from the value zero at each rod, the solution will resemble a sine function.

A second boundary condition is that the solution must be periodic as one goes from cell to cell, as we will see shortly. Since the total interaction potential has the same symmetry as the underlying lattice it can be expanded in terms of the reciprocal lattice vectors (RLVs) $\mathbf{G}$ as[22]

$$V(\boldsymbol{\rho}) = \sum_{\mathbf{G}} e^{i\mathbf{G}\cdot\boldsymbol{\rho}} V(\mathbf{G}), \tag{12}$$

where we define the Fourier coefficients of the interaction potential as

$$\begin{aligned} V(\mathbf{G}) &= \frac{1}{S}\int_S d^2\boldsymbol{\rho} e^{-i\mathbf{G}\cdot\boldsymbol{\rho}} V(\mathbf{r}) \\ &= -\frac{k_B T w_0}{S}\int_S d^2\boldsymbol{\rho} e^{-i\mathbf{G}\cdot\boldsymbol{\rho}} \sum_i K_0(\kappa|\boldsymbol{\rho}-\boldsymbol{\rho}_i|) \\ &= -\frac{k_B T w_0}{S}\int_S d^2\boldsymbol{\rho} \sum_i e^{-i\mathbf{G}\cdot\boldsymbol{\rho}_i} e^{-i\mathbf{G}\cdot(\boldsymbol{\rho}-\boldsymbol{\rho}_i)} K_0(\kappa|\boldsymbol{\rho}-\boldsymbol{\rho}_i|), \end{aligned} \tag{13}$$

where $S$ is the total area of the system perpendicular to the long axes of the macroions. Taking into account that on summing over a lattice of $\mathcal{M}$ sites $\boldsymbol{\rho}_i$ one has

$$\sum_i e^{-i\mathbf{G}\cdot\boldsymbol{\rho}_i} = \mathcal{M}, \tag{14}$$

it follows that

$$\begin{aligned} V(\mathbf{G}) &= -k_B T w_0 \frac{\mathcal{M}}{S}\int_S d^2\boldsymbol{\rho} e^{-i\mathbf{G}\cdot\boldsymbol{\rho}} K_0(\kappa|\boldsymbol{\rho}|) \\ &= -k_B T w_0 \frac{\mathcal{M}}{S}\frac{2\pi}{G^2+\kappa^2}. \end{aligned} \tag{15}$$

Hence the interaction potential has only Fourier components with inverse lattice vectors. Moreover the total strength of the macroion-polyelectrolyte interaction $w_0\mathcal{M}/S$ obviously depends on the macroion density. We will comment on this as we proceed.

The periodicity of the interaction potential has to be taken into account also in the Schrödinger equation in a way completely analogous to the case of electrons in a crystal.[22] The Schrödinger equation has a solution

$$\psi_{n\mathbf{k}}(\boldsymbol{\rho}) = e^{i\mathbf{k}\cdot\boldsymbol{\rho}} u_{n\mathbf{k}}(\boldsymbol{\rho}), \tag{16}$$

where by Floquet's theorem for any lattice vector $\mathbf{R}$ the function $u_{n\mathbf{k}}(\boldsymbol{\rho})$ is periodic

$$u_{n\mathbf{k}}(\boldsymbol{\rho}+\mathbf{R}) = u_{n\mathbf{k}}(\boldsymbol{\rho}), \tag{17}$$

and can thus be expanded in terms of the RLVs as

$$u_{n\mathbf{k}}(\boldsymbol{\rho}) = \sum_{\mathbf{G}} e^{i\mathbf{G}\cdot\boldsymbol{\rho}} u_n(\mathbf{G}). \tag{18}$$

Note that $u_{n\mathbf{k}}(\boldsymbol{\rho}=0)=0$ to satisfy the $\psi(\boldsymbol{\rho}=0)=0$ boundary condition. This leads straightforwardly to

$$\sum_{\mathbf{G}} u_n(\mathbf{G}) = 0. \tag{19}$$

As already alluded to for long chains, the dominant contribution to the partition function comes from the lowest-lying eigenvalue, which we assume corresponds to the ground state with $\mathbf{k}=0$. Therefore, in the limit of very long chains we only consider

$$\psi_n(\boldsymbol{\rho}) = \sum_{\mathbf{G}} e^{i\mathbf{G}\cdot\boldsymbol{\rho}} u_n(\mathbf{G}). \tag{20}$$

This ansatz leads to a Schrödinger equation of the form

$$\frac{\ell^2}{6}G^2 u_n(\mathbf{G}) + \beta\sum_{\mathbf{G}'} V(\mathbf{G}-\mathbf{G}') u_n(\mathbf{G}') = E_n u_n(\mathbf{G}), \tag{21}$$

or, if we take into account the form of the interaction potential in reciprocal space,

$$\begin{aligned} E_n u_n(\mathbf{G}) = \sum_{\mathbf{G}'} &\left(\frac{\ell^2}{6}G^2\delta_{\mathbf{G},\mathbf{G}'} - 2\pi\frac{\mathcal{M}}{S}\frac{w_0}{|\mathbf{G}-\mathbf{G}'|^2+\kappa^2}\right) \\ &\times u_n(\mathbf{G}'), \end{aligned} \tag{22}$$

where $\delta_{\mathbf{G},\mathbf{G}'}$ is the Kronecker delta. The similarities with the theory of electrons in a crystal[22] are now even more apparent. The only difference is that for polyelectrolytes we restrict ourselves to the $\mathbf{k}=0$ solution, and the interaction potential is of a screened Debye–Hückel type as opposed to standard Coulomb potential. The solution of the above equation clearly depends on the symmetry of the reciprocal lattice. Let us now assume that the macroions are arranged in a 2D hexagonal lattice with lattice spacing $R$, where the real space basis is

$$\begin{aligned} \mathbf{a}_1 &= R\mathbf{i} \\ \mathbf{a}_2 &= \frac{R}{2}(\mathbf{i}+\sqrt{3}\mathbf{j}), \end{aligned} \tag{23}$$

so the unit cell area is $S/\mathcal{M} = \mathbf{a}_1\times\mathbf{a}_2 = R^2\sqrt{3}/2$. The RLVs can then be written as

$$\mathbf{G} = n_1\mathbf{b}_1 + n_2\mathbf{b}_2, \tag{24}$$

where $n_1$, $n_2$ are integers and the basis vectors are given by

$$\begin{aligned} \mathbf{b}_1 &= \frac{2\pi}{R\sqrt{3}}(\sqrt{3}\mathbf{i}-\mathbf{j}), \\ \mathbf{b}_2 &= \frac{2\pi}{R\sqrt{3}}2\mathbf{j}. \end{aligned} \tag{25}$$

The square of the RLV $\mathbf{G}$ is thus

$$G^2 = \left(\frac{2\pi}{R}\right)^2\frac{4}{3}(n_1^2+n_2^2-n_1n_2). \tag{26}$$

TABLE I. First several sets of reciprocal lattice vectors (RLVs). We only use compound indices 0–18 in the main text.

| Set | $(n_1,n_2)$ | $n_1^2+n_2^2-n_1n_2$ | Compound index |
|---|---|---|---|
| 1 | $(0,0)$ | 0 | 0 |
| 2 | $(1,0)(1,1)(0,1)(\bar{1},0)(\bar{1},\bar{1})(0,\bar{1})$ | 1 | 1–6 |
| 3 | $(1,\bar{1})(\bar{1},1)(2,1)(1,2)(\bar{1},\bar{2})(\bar{2},\bar{1})$ | 3 | 7–12 |
| 4 | $(2,0)(0,2)(\bar{2},0)(0,\bar{2})(\bar{2},\bar{2})(2,2)$ | 4 | 13–18 |
| 5 | $(2,\bar{1})(\bar{1},2)(\bar{2},1)(1,\bar{2})(3,\bar{1})(\bar{1},3)$ $(3,\bar{1})(\bar{1},3)(3,2)(2,3)(3,\bar{2})(\bar{2},3)$ | 7 | 19–30 |
| … | … | … | … |

The RLVs can now be ordered into sets according to their magnitude. A few of the lowest-lying sets are given in Table I, together with the magnitude of the corresponding reciprocal lattice vector and the compound indices used later for bookkeeping purposes. In what follows we will find numerical, and in one case analytical, solutions for the eigenvalue systems defined by compound indices (0–6), (0–12), and finally for (0–18). The first set of compound indices corresponds to the central "point" together with its six first neighbors, the second one to the additional six next nearest neighbors and the last one to the final six next-next nearest neighbors.

These solutions will give us an idea of how the eigenvalues and, in particular, the smallest eigenvalue behave as a function of the lattice spacing. In what follows we will measure energies relative to $\beta V(\mathbf{G}=0)$. The Schrödinger equation (Eq. (22)) for the first two sets of RLVs (see Table I) with compound indices (0–6) leads to the following $7\times 7$ set of eigenvalue equations:

$$
\begin{aligned}
Eu_0 &= -\beta V(G_2)(u_1+u_2+u_3+u_4+u_5+u_6),\\
Eu_1 &= \frac{\ell^2}{6}G_2^2u_1-\beta V(G_2)(u_0+u_2+u_6)-\beta V(G_3)(u_3+u_5)\\
&\quad -\beta V(G_4)u_4,\\
Eu_2 &= \frac{\ell^2}{6}G_2^2u_2-\beta V(G_2)(u_0+u_1+u_3)-\beta V(G_3)(u_4+u_6)\\
&\quad -\beta V(G_4)u_5,\\
Eu_3 &= \frac{\ell^2}{6}G_2^2u_3-\beta V(G_2)(u_0+u_2+u_4)-\beta V(G_3)(u_1+u_5)\\
&\quad -\beta V(G_4)u_6,\\
Eu_4 &= \frac{\ell^2}{6}G_2^2u_4-\beta V(G_2)(u_0+u_3+u_5)-\beta V(G_3)(u_2+u_6)\\
&\quad -\beta V(G_4)u_1,\\
Eu_5 &= \frac{\ell^2}{6}G_2^2u_5-\beta V(G_2)(u_0+u_4+u_6)-\beta V(G_3)(u_1+u_3)\\
&\quad -\beta V(G_4)u_2,\\
Eu_6 &= \frac{\ell^2}{6}G_2^2u_6-\beta V(G_2)(u_0+u_1+u_5)-\beta V(G_3)(u_2+u_4)\\
&\quad -\beta V(G_4)u_3,
\end{aligned}
\tag{27}
$$

where the four RLVs corresponding to the first two sets of Table I are given by $G_1=0$, $G_2=2\pi/R\sqrt{\frac{4}{3}}$, $G_3=\sqrt{3}2\pi/R\sqrt{\frac{4}{3}}$, $G_4=2\,2\pi/R\sqrt{\frac{4}{3}}$. Also we have here $V(G)=2\pi\mathcal{M}/S\,w_0/|\mathbf{G}-\mathbf{G}'|^2+\kappa^2$. Thus the lowest-lying energy $E$ is obtained from the determinant of the following matrix

$$
\begin{bmatrix}
E & \beta V(G_2) & \beta V(G_2) & \beta V(G_2) & \beta V(G_2) & \beta V(G_2) & \beta V(G_2)\\
\beta V(G_2) & E-\frac{\ell^2}{6}G_2^2 & \beta V(G_2) & \beta V(G_3) & \beta V(G_4) & \beta V(G_3) & \beta V(G_2)\\
\beta V(G_2) & \beta V(G_2) & E-\frac{\ell^2}{6}G_2^2 & \beta V(G_2) & \beta V(G_3) & \beta V(G_4) & \beta V(G_3)\\
\beta V(G_2) & \beta V(G_3) & \beta V(G_2) & E-\frac{\ell^2}{6}G_2^2 & \beta V(G_2) & \beta V(G_3) & \beta V(G_4)\\
\beta V(G_2) & \beta V(G_4) & \beta V(G_3) & \beta V(G_2) & E-\frac{\ell^2}{6}G_2^2 & \beta V(G_2) & \beta V(G_3)\\
\beta V(G_2) & \beta V(G_3) & \beta V(G_4) & \beta V(G_3) & \beta V(G_2) & E-\frac{\ell^2}{6}G_2^2 & \beta V(G_2)\\
\beta V(G_2) & \beta V(G_2) & \beta V(G_3) & \beta V(G_4) & \beta V(G_3) & \beta V(G_2) & E-\frac{\ell^2}{6}G_2^2
\end{bmatrix}.
\tag{28}
$$

The seven eigenvalues of the matrix Eq. (28) can be found analytically and are given by

$$
E_{1,2}=\frac{\ell^2}{6}G_2^2+\beta V(G_2)+\beta V(G_3)-\beta V(G_4),
$$

$$E_3 = \frac{\ell^2}{6}G_2^2 + 2\beta V(G_2) - 2\beta V(G_3) + \beta V(G_4),$$

$$E_{4,5} = \frac{\ell^2}{6}G_2^2 - \beta V(G_2) + \beta V(G_3) + \beta V(G_4), \tag{29}$$

$$E_{6,7} = \left[\frac{\ell^2}{6}G_2^2 - 2\beta V(G_2) - 2\beta V(G_3) - \beta V(G_4)\right]\left(1 \pm \sqrt{\frac{24\beta V(G_2)^2}{\left[\frac{\ell^2}{6}G_2^2 - 2\beta V(G_2) - 2\beta V(G_3) - \beta V(G_4)\right]^2}}\right).$$

Their dependence on $R$ is shown in Fig. 2. In the limit of large $R$ the lowest eigenvalue is degenerate and equal to $E_{4,5}$. The eigenvectors corresponding to it satisfy the condition of Eq. (19), which stems from the impenetrability of the macromolecular rods on the lattice sites, approximated as infinitely thin cylinders. Other eigenvectors do not satisfy Eq. (19), but additional solutions can be obtained by taking linear combinations of higher-energy eigenvectors, with relative amplitudes chosen to satisfy Eq. (19). The corresponding eigenenergies are then given by appropriate weighings of the associated eigenvalues.

It is instructive to investigate the lowest-lying eigenvalue in the limiting cases of either $R \to 0$ or $R \to \infty$, respectively. We find from Eq. (29) that in these two limits

$$E_{4,5}(R \to 0) \to \frac{8\pi^2}{9}\frac{\ell^2}{R^2},$$

$$E_{4,5}(R \to \infty) \to -\left(\frac{64 w_0 \mathcal{M}\pi^2}{S\kappa^2} - \frac{8(\kappa\ell)^2\pi^2}{9}\right)\frac{1}{(\kappa R)^2}. \tag{30}$$

For small values of $R$ the lowest-lying eigenvalue scales as $R^{-2}$. For ground-state dominance, where the lowest-lying eigenvalue is related to the free energy of the polyelectrolyte chain [see Eq. (11)], this means that the polyelectrolytes add a repulsive contribution to the interactions between the macroions. In the opposite limit of large values of $R$ but simultaneously with large values of the strength of interaction $w_0$, the interactions are attractive, as can be again seen from Eq. (30), and scale as $-R^{-2}$. The sign of the asymptotic form of the lowest-lying eigenenergy depends on the value of $w_0$. There is a critical value $w_0 = w_c$, above which the lowest-lying eigenvalue becomes negative. Attractions are thus seen only for $w_0 > w_c$ (see Fig. 3). In the asymptotic limit of Eq. (30) the critical value of $w_0$ is seen to be

$$w_c = \frac{(\kappa\ell)^2\kappa^2}{72\frac{\mathcal{M}}{S}}, \tag{31}$$

and is obviously a function of the ionic strength of the medium. The critical value $w_c$ also strongly depends on the partial set of RLVs and converges slowly, just like the eigenvalues themselves (see below). Its exact value would be thus difficult to evaluate in the reciprocal space analysis. A better and faster estimate can be obtained from the WKB ansatz to be discussed shortly.

Let us next analyze the monomer density distribution given by $\rho(|\boldsymbol{\rho}|) = \psi^2(|\boldsymbol{\rho}|)$, for the lowest-lying eigenvalue at small and large values of $R$, $R = 3$ Å and $R = 30$ Å for RLV set (0–6). We first consider small $R$, depicted on the left part of Fig. 4. Here the polymer density is mostly concentrated in the interstitial regions of the hexagonal lattice, with no overlap between different lattice sites. For small $R$ the polymer is thus squeezed in the interstices between lattice sites leading to repulsion in the total free energy (positive eigenenergy). This steric effect is due to the boundary condition of vanishing monomer density at the surface of the macroion, or in the limit of small macroion size, vanishing density at the lattice sites, $\psi(|\boldsymbol{\rho}| = 0) = 0$. An analogous distribution of monomer density is observed also in the 1D case[11] at small intersurface separations. We now consider large $R$, depicted on the right part of Fig. 4. Here a different type of monomer density distribution occurs, where the monomers tend to concentrate around the lattice sites, away from interstitial regions, with nonnegligable density between lattice sites. This means that parts of the chains span the regions between lattice sites in a bridging configuration. The eigenenergy corresponding to these bridging configurations is negative, leading to attractive interactions. Again the situation is completely analogous to bridging in the 1D case for large intersurface separations.[11]

Let us delve a bit also into the other two sets of compound indices [they are (0–12) and (0–18) as defined in Table I] for which no analytical solution to the eigenvalue problem exists and we obtain only numerical solutions for the eigenenergies presented on Figs. 5 and 6. The qualitative behavior of the lowest-lying energy eigenvalue is exactly the same as for the first set of compound indices (see Fig. 2). The lowest-lying energy eigenvalue starts from a large positive value at small $R$, then goes through zero for a finite $R$ and finally becomes negative with a minimum at intermediate values of $R$. The asymptotic behavior of the lowest-lying eigenvalue always seems to follow the $R^{-2}$ form irrespective of the choice of the basis set.

By comparing the eigenvalue behavior on Figs. 2, 5, and 6, we see that the above method of consecutive construction of eigenvalues with partial sets of reciprocal wave vectors converges very slowly. Although one could in principle con-

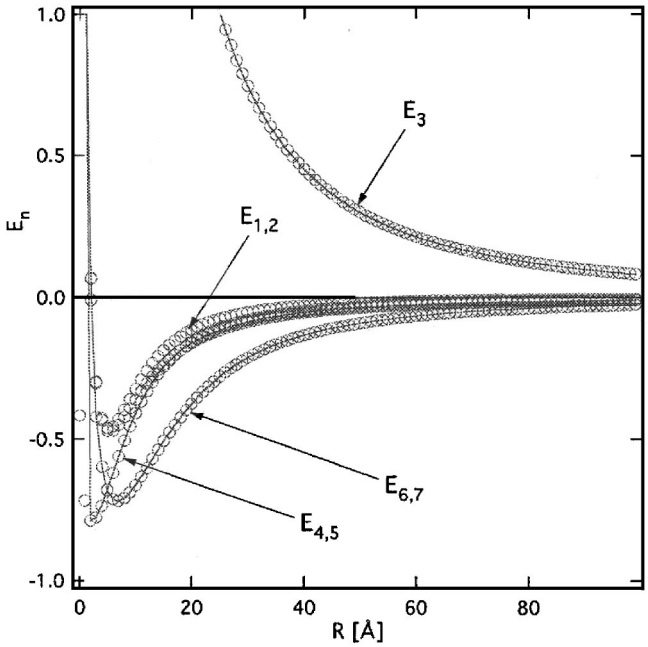


FIG. 2. Energy eigenvalues of the first two sets of RLV characterized by the compound indices (0–6) (see Table I), as a function of the lattice constant $R$. In this case, and only in this case, can the energy eigenvalues be derived also analytically (see main text). On all figures, unless indicated otherwise, we have taken $1/\kappa=1$ Å, $\ell=1$ Å, $w_0\mathcal{M}/\kappa^2 S=1$, so that $w_0$ is way above the critical value $w_c$ [see Eq. (31)].

tinue this line of reasoning by going to progressively larger sets of RLVs, it is desirable to have even an approximate analytical asymptotic form of the lowest-lying energy eigenvalue in place of detailed numerical computations. In the next sections we will explore the possibilities of obtaining these forms.

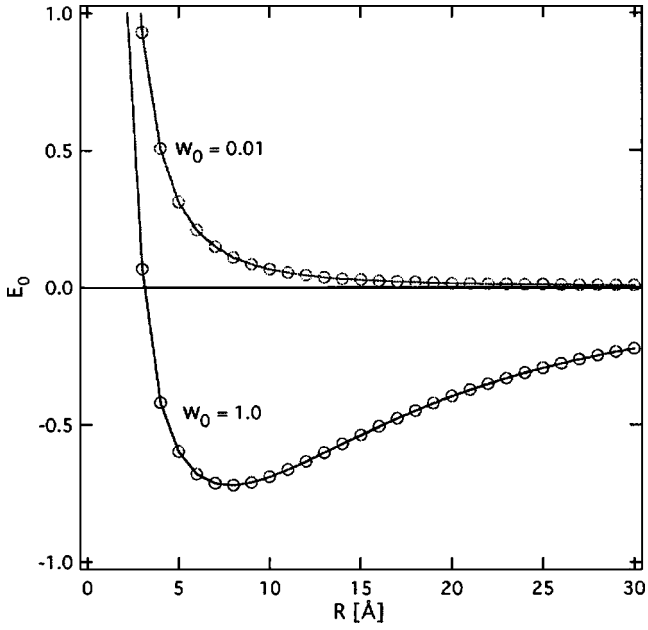


FIG. 3. Lowest-lying energy eigenvalues of the set of RLVs characterized by the compound indices (0–6) (see Table I) as a function of the lattice constant $R$ for subcritical ($w_0=0.01$) and supercritical ($w_0=1$) value of $w_0$. In the subcritical case the attractive part of the curve is clearly missing. The exact critical value of $w_0$ could be obtained only with time consuming numerical search and would depend on the RLV basis set.

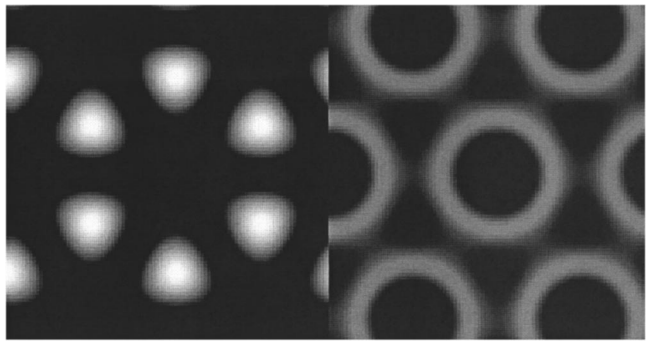

FIG. 4. Monomer density profile (bright regions correspond to high density) for RLV set (0–6) and for eigenfunctions corresponding to lowest-energy eigenvalue at two different values of the lattice constant ($R=3$ Å and $R=30$ Å with $w_0=1$), rescaled so that the whole unit cell is shown in both cases. For small $R$ (left) the monomer density is confined to the lattice interstitial regions, given by the triangle centers at $\pm(30,90,150)$ degrees from the $x$ axis. The energy eigenvalue here is positive, corresponding to repulsive interactions. For large $R$ (right) the monomer density consists of circular distributions centered around each lattice point, with a small density increase (bridging) along the lines joining the lattice points, which are at $\pm(0,60,120)$ degrees to the $x$ axis.

The most important drawback of the above calculation is that we did not take into account the fact that the compound magnitude of the macroion-polyelectrolyte interaction, $w_0\mathcal{M}/S$, explicitly depends on the macroion density or $R$. In principle that could also be taken into account but the price one would have to pay is that it would be much more difficult to identify the lowest-lying eigenvalue and derive its analytical properties in terms of dependence on $R$. This is due to the fact that the magnitude of interactions would vary with $R$ and for different values of $R$ different energy eigenvalues would be minimal. Rather then making the above cal-

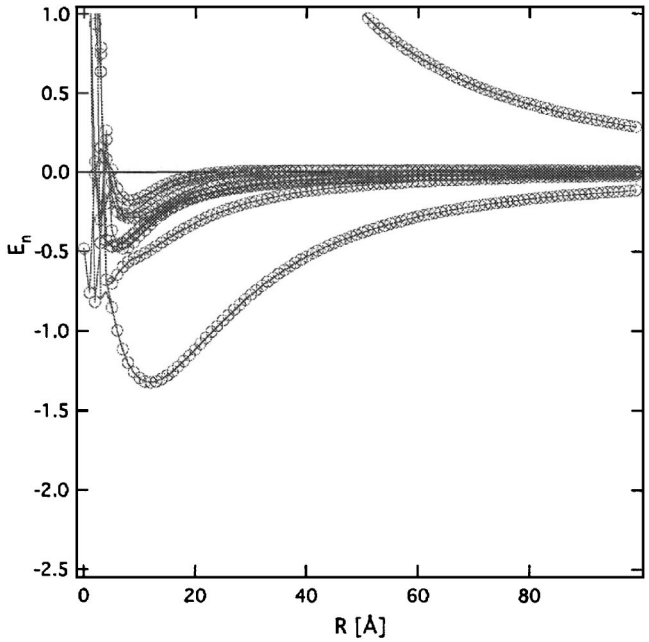


FIG. 5. Energy eigenvalues of the set of RLV characterized by the compound indices (0–12) (see Table I), as a function of the lattice constant $R$. It is clearly discernible that the difference between the lowest-lying eigenvalue and the rest is becoming larger. This trend persists as one augments the RLV basis set.

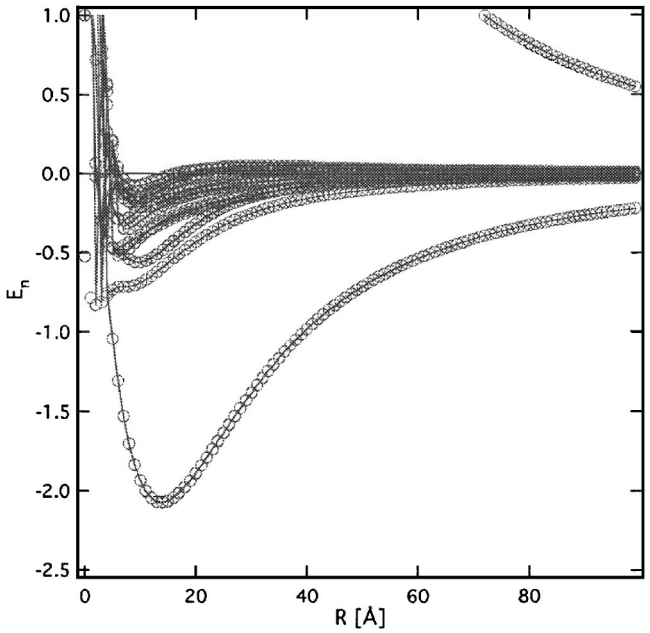


FIG. 6. Energy eigenvalues of the set of RLV characterized by the compound indices (0–18) (see Table I) as a function of the lattice constant $R$. It is again discernible that the difference between the lowest-lying eigenvalue and the rest is becoming larger.

culation less transparent and in fact resorting to heavy numerics, while nevertheless still remaining limited by the slow convergence of the results in the RLV space, we proceed by a more complete analysis on the Wigner–Seitz cell level, addressed next.

## IV. WIGNER–SEITZ APPROXIMATION

Let us now consider the Wigner–Seitz approximation, commonly employed in the theory of electrons in crystals.[22] Here one deals with a single cylindrical cell instead of a periodic array. In our case the cell area is set by the macroion density, and the periodicity of the wave function across the array is simulated by an appropriate boundary condition at the edge of the cell. The effective strength of interaction does not depend on the macroion density anymore.

We thus must solve the following equation within the cylindrical cell, of radius $R' = \sqrt{\sqrt{3}/2\pi}R$, chosen so that $\pi R'^2 = S/\mathcal{M}$:

$$\left[ -\frac{\ell^2}{6}\nabla_\perp^2 - w_0 K_0(\kappa\rho) \right] \psi(\rho) = E\psi(\rho). \tag{32}$$

There are two boundary conditions (BCs). One is at the inner wall of the cell, coinciding with the surface of the macroion, where the polymer boundary condition enforces the solution $\psi(\rho)$ to take the value zero. Again if one approximates the macroions with thin rods this BC reduces to $\psi(0)=0$. The second BC is that the solution from one Wigner–Seitz cell should smoothly connect with the solution in the neighboring cell. This is mimicked by the BC that the normal derivative of the solution at the outer wall has to vanish. Thus

$$\psi(0) = 0, \quad \mathbf{n}\cdot\boldsymbol{\nabla}\,\psi(R') = 0. \tag{33}$$

Since by symmetry the wave function can depend only on coordinate $\rho$ we have *in extenso*

$$\left[ -\frac{\ell^2}{6}\frac{1}{\rho}\frac{d}{d\rho}\left(\rho\frac{d\psi}{d\rho}\right) - w_0 K_0(\kappa\rho) \right] \psi(\rho) = E\psi(\rho). \tag{34}$$

This equation, subject to the zero value BC at $|\boldsymbol{\rho}|=0$ and zero slope BC at $|\boldsymbol{\rho}|=R'$, gives us the complete solution on the Wigner–Seitz level. Unfortunately, simplified as this approach already is, it is solvable only numerically. We shall postpone a detailed numerical analysis of this equation and the ensuing eigenvalue for a later publication and analyze here only its salient asymptotic behavior.

We can, however, make some general comments. On moving away from the rod, $\psi$ develops a nonzero amplitude, but has a negative curvature tending to bend it back to zero. The lowest-energy solution is the one where the wave function bends back to zero only once in order to match the zero-slope Wigner–Seitz BC at the outer wall. A simple and intuitive solution occurs for small values of $w_0$, where the potential matters only for small $\rho$. In that case the large $K_0(\kappa\rho)$ factor forces negative curvature on the eigenfunction, which is, however, not enough to curve the solution downwards to satisfy the boundary condition $d\psi(\rho)/d\rho|_{\rho=R'}=0$. This can only be achieved if in addition the eigenenergy is sufficiently large and positive. If $R'$ is increased at fixed eigenvalue $E$, the wave function will overshoot the boundary; hence, to match the boundary condition at the larger $R'$, the eigenenergy $E$ must decrease because this decreases the curvature. For most $\rho$ the potential will be ineffective. Hence the free-space solution will dominate. It has the form $\psi(\rho) \sim \sin k\rho/\sqrt{\rho}$, where $kR' = \pi/2$ to ensure the second BC that $\psi(R')$ has zero slope (neglecting the $\sqrt{\rho}$ term) at the outer boundary and the sin was taken to ensure the first BC at the origin. The corresponding eigenvalue is thus

$$E = \frac{(\pi l)^2}{24R'^2}. \tag{35}$$

For finite $w_0$ there is no intuitively straightforward argument that would describe the general properties of the ensuing solution.

## V. WKB SOLUTION TO THE WIGNER–SEITZ APPROXIMATION

Before solving Eq. (32) numerically, we will first invoke the WKB method, an analytical approach that has already proved useful in the context of polyelectrolyte bridging interactions.[11] This will allow us to find accurate analytical approximation and asymptotics which is indeed what we are after.

Let us summarize the general features of the bridging interaction in the related 1D case,[11] involving two charged planes with a polymer chain in between. There the polymer density was zero at each plane and the slope was zero at their midpoint because of symmetry constraints. Two regimes were found. For small (large) separation between the planes relative to the screening length, the polymer density had a maximum (minimum) at the midplane, leading to prevailing steric repulsions or bridging attractions (for details see the discussion in Ref. 11). In the present lattice problem the

Wigner–Seitz cell corresponds roughly to one-half the confining space between the plates in the 1D case. Depending on the spacing between the macroions the polymer density will by analogy have a maximum (minimum) at the edge of the cell for small (large) macroion separations leading again to repulsive (attractive) interactions. Most of the physics of the 1D case is thus strictly preserved in the 2D case, which is both surprising and encouraging.

First we rewrite the Schrödinger equation in terms of the new variable $x=\log \rho$. It reads

$$\frac{d^2\psi(x)}{dx^2} + \frac{G}{\ell^2}[E + w_0 K_0(\kappa e^x)]e^{2x}\psi(x) = 0, \tag{36}$$

allowing for a very straightforward application of the standard WKB formalism.[24] Depending on the sign of $E + w_0 K_0(\kappa e^x)$ the WKB solution has two standard forms. To see this we revert back to the original variable $\rho$, and introduce the auxiliary function

$$g(\rho) = \frac{6}{\ell^2}[E + w_0 K_0(\kappa\rho)]. \tag{37}$$

In terms of $g(\rho)$, the two types of solution can be written as

$$\psi(\rho) \sim [g(\rho)\rho^2]^{-1/4} \exp[\pm i \int^{\rho} g(\rho)^{1/2} d\rho], \quad g(\rho) > 0,$$
$$\psi(\rho) \sim [-g(\rho)\rho^2]^{-1/4} \exp\{\pm \int^{\rho} [-g(\rho)]^{1/2} d\rho\}, \quad g(\rho) < 0. \tag{38}$$

As indicated above the wave function $\psi(\rho)$ should be zero at the center of the cell and have zero slope at the outer boundary of the cell, or

$$\psi(\rho = 0) = 0$$

and

$$\left.\frac{d\psi(\rho)}{d\rho}\right|_{\rho=R'} = 0. \tag{39}$$

These two BCs and Eq. (36) allow us to calculate the energy eigenvalue in the standard manner. Consider $\kappa$ and $l$ to be fixed. The lowest eigenvalue $E$ is still a function of $w_0$ and $R'$: $E=E(w_0,R')$. At fixed $R'$ let us consider the effect of increasing $w_0$ from 0, where $E$ is given by Eq. (35). By Eq. (36), to maintain the same average curvature integrated over $\rho$, an increase in $w_0$ should be accompanied by a decrease in $E$. For $E>0$ (so $w_0$ is not too large), at fixed $w_0$ let us now consider the effect of increasing $R'$. By Eq. (36), to maintain the same average curvature integrated over $\rho$, an increase in $R'$ should be accompanied by a decrease in $E$. Thus the system tends to self-repel. For some critical value $w_c(R')$ of $w_0$, the system attains the value $E=0$. For larger $w_0$, so $E<0$, the behavior can be more complex, because for large $\rho$ the curvature can become positive (i.e., dominated by negative $E$). In this case, for a given value of $w_0$, there is a value of $R'$ beyond which $E$ becomes less negative as $R'$ increases. We will see this behavior in what follows. The equilibrium value $R_0(w_0)$ of $R'$ occurs for $dE/dR'=0$.

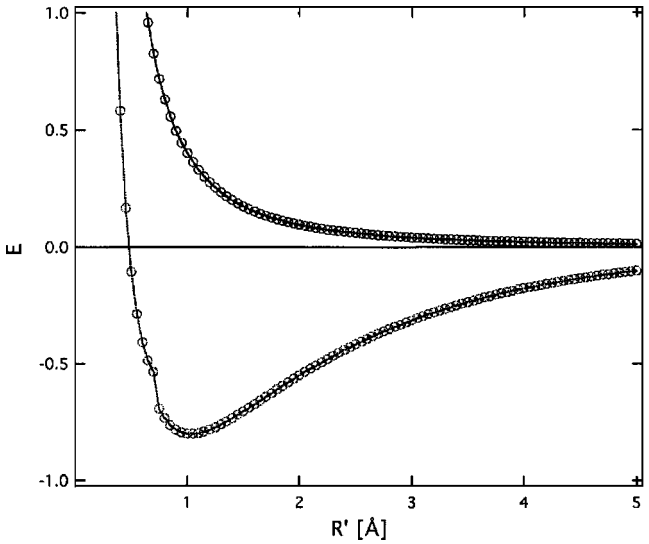


FIG. 7. Energy eigenvalues $E(R')$ obtained with the WKB method in the Wigner–Seitz model. The upper curve is for $w_0=0.01$ and the lower curve is for $w_0=1.0$. The qualitative form of the eigenvalue as a function of $R'$ is very similar to the one obtained from the reciprocal lattice method. All the parameters are taken the same as in the reciprocal lattice case.

Using the parameters $1/\kappa=1$ Å and $\ell=1$ Å, Fig. 7 presents two families of ground-state eigenvalues ($w_0=0.01$ and $w_0=1.0$) as functions of $R'$. As expected, the curve for larger $w_0$ has the smaller $E$. The two $E(R')$ curves have the same qualitative characteristics as the corresponding solutions in Fig. 5, obtained by solving the Schrödinger equation in reciprocal lattice space. In this case, however, we explicitly consider the complete $R'$ dependence of the eigenvalue.

These curves also show that, as indicated above, for sufficiently large $w_0$ the eigenenergy becomes negative. This indicates a binding, i.e., a bridging attraction. For the small value $R'=3$ Å, the corresponding monomer density is presented on the left-hand side of Fig. 8, and shows sterically confined polymer chains with a maximum in the density precisely at the outer wall of the WS cell. For the large value $R'=30$ Å, presented on the right-hand side of Fig. 8, the density maximum is displaced to the interior of the cell with finite but small density of the polymer at the outer wall of the

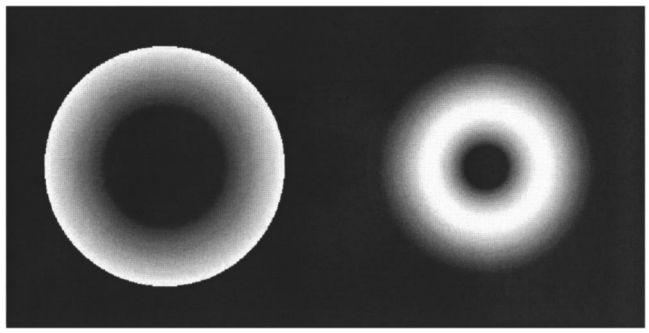

FIG. 8. Monomer density profile for Wigner–Seitz WKB approximation with $w_0=1$, for two WS radii ($R'=3$ on the left and $R'=30$ on the right), rescaled so that the whole unit cell is shown in both cases. For small $R'$ the configurations are confined, with most of the chain at the outer wall of the cell, whereas for large $R'$ there again are bridging configurations, with a density maximum in the interior of the cell. The two density profiles represent WKB Wigner–Seitz approximations to the lattice calculations, Fig. 4.

WS cell. This distribution of the chain corresponds to bridging configurations where the finite monomer density at the outer wall simulates chain bridging between neighboring cells. Qualitatively the state of affairs is exactly the same as in the reciprocal lattice space calculation. All this is again completely analogous to the 1D case,[11] where at small separations between the plates the polymer accumulates in the middle of the intersurface space, leading to repulsive interactions, or close to the plates, leading to bridging attractions.

In order to derive analytical estimates for $E=E(w_0,R')$ from the WKB ansatz, we will proceed separately for the two cases where $g(\rho)>0$ for all $\rho$ (as occurs for $E>0$) and where $g(\rho)<0$ for large enough $\rho$ (as occurs for $E<0$).[24]

### A. Solution if $g(\rho)>0$ for all $0<\rho<R'$

For $g(\rho)>0$ one has $|E|<w_0K_0(\kappa\rho)$ in the whole interval $0<\rho<R'$. As indicated above, this does not necessarily imply that $E>0$ and one can thus have repulsive as well as attractive polyelectrolyte-mediated interactions. Let us take a closer look at this solution. The BC at the center of the Wigner–Seitz cell sets the WKB wave function to be of the form

$$\psi(\rho)\sim[g(\rho)\rho^2]^{-1/4}\sin\left[\int_0^\rho g(\rho)^{1/2}d\rho\right]. \tag{40}$$

Taking into account the zero-slope boundary condition at $\rho=R'$, the phase of the sine of the argument in Eq. (40) is $\pi/2$, so

$$\int_0^{R'}\sqrt{E+w_0K_0(\kappa\rho)}d\rho=\frac{\pi}{2}\sqrt{\frac{\ell^2}{6}}. \tag{41}$$

This may be written in dimensionless form as

$$\int_0^{\kappa R'}\sqrt{\frac{E}{w_0}+K_0(u)}du=\frac{\pi}{2}\sqrt{\frac{(\kappa\ell)^2}{6w_0}}. \tag{42}$$

In principle, this gives $E/w_0=F(\kappa R',(\kappa\ell)^2/w_0)$. The critical value $w_c(R')$ of $w_0$, where $E=0$, is obtained on setting $0=F[\kappa R',(\kappa\ell)^2/w_c]$.

There is no closed form analytical solution to Eq. (42) since the integral on the left-hand side cannot be reduced to elementary quadratures. There are nevertheless a few limiting cases that can be dealt with explicitly. First note that the $E=0$ line separates bridging configurations from nonbridging configurations. We have already encountered this phenomenon in the reciprocal lattice calculation where a critical value $w_c$ separated the case with no attractions (nonbridging configurations) and the case with finite attractions (bridging configurations). In the above WKB limit we are able to obtain an approximate value for $w_c$ in the following way. The branching point is defined by $E=0$ and $w_0=w_c$, thus leading to

$$\int_0^{R'}\sqrt{w_0K_0(\kappa\rho)}d\rho=\frac{\pi}{2}\sqrt{\frac{\ell^2}{6}}. \tag{43}$$

This equation has a solution only for $w_0\geq\pi^2/24\times2.11955^2(\kappa\ell)^2\approx0.0915(\kappa\ell)^2$. The branching point is thus defined by

$$w_c=(\mu/e)_c\ell_B\approx\frac{\pi^2}{0.1}(\kappa\ell)^2. \tag{44}$$

The WKB solution thus allows us to compute the critical ratio of the charge per unit length of the macroion $\mu$ and charge per segment of the polyelectrolyte $e$ that allows for bridging configurations. For any $w_0>w_c$ there will be a regime of $R'$ with bridging configurations. This is all very similar to the 1D case.[11]

One cannot, however, compare Eq. (30) with the limit [Eq. (44)] directly, since in the former case we assumed that the effective strength of the interaction is macroion density independent. The result in Eq. (44) thus presents the correct form of the condition for the branching point in the solution.

Let us now try to extract some limiting laws from the WKB solution [Eq. (41)]. For small $w_0$, Eq. (41) leads to the expression

$$\int_0^{R'}\sqrt{E+w_0K_0(\kappa\rho)}d\rho\simeq\sqrt{E}R'+\frac{w_0}{2\sqrt{E}}\int_0^{R'}K_0(\kappa\rho)d\rho+\cdots=\frac{\pi}{2}\sqrt{\frac{\ell^2}{6}}. \tag{45}$$

Thus we furthermore have

$$E(R)\simeq\left(\frac{\pi}{2}\right)^2\frac{\ell^2}{6R^2}\left(1+\tfrac{1}{2}\sqrt{1-\alpha(R')}-\tfrac{1}{4}[2+\alpha(R')]\right), \tag{46}$$

where

$$\alpha(R')=\frac{12w_0}{\left(\frac{2}{\pi}\right)^2(\kappa\ell)^2}(\kappa R')\int_0^{\kappa R'}K_0(u)du. \tag{47}$$

From this we conclude that for weak enough electrostatic attractions between macroions and flexible polyelectrolyte chains, i.e., for sufficiently small $w_0$, the electrostatic effects are only a perturbation to dominant steric effects. Note that Eq. (47) reduces to Eq. (35) as $w_0\to0$, as expected.

### B. Solution if $g(\rho)<0$ for some $0<\rho<R'$

Here again our analysis follows the analogous 1D case.[11] For $E+w_0K_0(\kappa\rho)<0$, the situation is more complicated than above. Clearly in this case one should have $|E|>w_0K_0(\kappa\rho)$ corresponding either to small $E<0$ with a weak (attractive) interaction characterized by $w_0$, or to a large enough cell that the interaction is well screened at the Wigner–Seitz radius $R'$.

In this case, for small $\rho$ the curvature of the wave function as deduced from the Schrödinger equation [Eq. (32)] is negative for small $\rho$, but positive for large $\rho<R'$. We will call the point $\rho_0$, where the curvature is zero, the classical turning point. It is the solution of

$$-|E|+w_0K_0(\kappa\rho_0)=0. \tag{48}$$

In principle this gives $\rho_0(w_0,E)$, but $E$ is not yet known, and the method of the previous subsection does not apply to the present case.

By neglecting the prefactor $g(\rho)^{-1/4}$, the WKB solution for small $\rho$ with zero value at $\rho=0$ varies as a sine, and for $\rho>\rho_0$ the solution is a sum of sines and cosines. The two solutions have to be continuous at the turning point, which gives us the necessary constants as they are typically obtained in the WKB framework.[24] Specifically,

$$\psi(\rho) \sim [w_0 K_0(\kappa\rho) - |E|]^{-1/4} \times \sin\left\{ \sqrt{\frac{6}{\ell^2}} \int_0^\rho [w_0 K_0(\kappa\rho) - |E|]^{1/2} d\rho \right\}, \quad 0 < \rho < \rho_0,$$

$$\psi(\rho) \sim [|E| - w_0 K_0(\kappa\rho)]^{-1/4} \left\{ e^{M_0} \sin\left[ \frac{\pi}{4} - \xi(\rho) \right] + e^{-M_0} \cos\left[ \frac{\pi}{12} + \xi(\rho) \right] \right\}, \quad \rho_0 < \rho < R', \tag{49}$$

where we introduce two auxiliary quantities

$$M_0 = \sqrt{\frac{6}{\ell^2}} \int_0^{\rho_0} [w_0 K_0(\kappa\rho) - |E|]^{1/2} d\rho,$$

$$\xi(\rho) = \sqrt{\frac{6}{\ell^2}} \int_{\rho_0}^{\rho} [|E| - w_0 K_0(\kappa\rho)]^{1/2} d\rho. \tag{50}$$

The sin term of the interior solution already takes into account the boundary condition at the origin $\rho=0$, while the boundary condition of zero slope at the outer boundary of the Wigner–Seitz cell has to be taken into account explicitly. This boundary condition at $\rho=R'$ reduces to

$$\cos\left[ \frac{\pi}{4} - \xi(R') \right] + e^{-2M_0} \sin\left[ \frac{\pi}{12} + \xi(R') \right] = 0. \tag{51}$$

As $M_0$ is strictly positive and varies from $+\infty$ to $+0$, the solution $\xi(R')$ of this equation varies from $3\pi/4$ to $5\pi/6$. In the general case, $\xi(R')$ can be obtained only numerically, although clearly it depends only weakly on $R'$. We can exploit this weak dependence on $R'$ and derive a closed form approximate analytical solution for the eigenenergy in the asymptotic regime of $R' \to \infty$.

To obtain this approximate solution we introduce the dimensionless variable $\kappa\rho=u$, with $\kappa R'=U$ and $\kappa\rho_0=u_0$. Then

$$M_0 = \sqrt{\frac{6w_0}{(\kappa\ell)^2}} \int_0^{u_0} [K_0(u) - K_0(u_0)]^{1/2} du,$$

$$\xi(R') = \sqrt{\frac{6w_0}{(\kappa\ell)^2}} \int_{u_0}^{U} [K_0(u_0) - K_0(u)]^{1/2} du. \tag{52}$$

In the asymptotic limit where we assume that $|E| \to 0$, we can approximate $K_0(u) \simeq \sqrt{\pi/2u} e^{-u}$ in the equation for $\xi$ and $K_0(u) \simeq -\log u/2 - \gamma$ in the equation for $M_0$. Then we expand $\xi$ in terms of $K_0(u)$ and $M_0$ in terms of $K_0(u_0)$. This reasoning leads to the following approximate forms:

$$M_0 \simeq \sqrt{\frac{6w_0}{(\kappa\ell)^2}} \int_0^{u_0} \left( \sqrt{-\log\frac{u}{2}} + \ldots \right) du = \sqrt{\frac{6w_0\pi}{(\kappa\ell)^2}} \{1 + \mathcal{O}[e^{(-u_0)}]\},$$

$$\xi(R') \simeq \sqrt{\frac{6w_0}{(\kappa\ell)^2}} \sqrt{\sqrt{\frac{\pi}{2u_0}} e^{-u_0}} \int_{u_0}^{U} (1 + \ldots) du = \sqrt{\frac{6w_0}{(\kappa\ell)^2}} \sqrt{\sqrt{\frac{\pi}{2u_0}} e^{-u_0}} \times \left\{ U - u_0 - \tfrac{1}{2} + \mathcal{O}[e^{-(u-u_0)}] \right\}. \tag{53}$$

We have taken into account above that both $U$ and $u_0$ are large in the asymptotic limit. From the boundary condition it now follows that $\xi$ is a function only of $M_0$, which itself is a function of $6w_0\pi/(\kappa\ell)^2$ and no longer depends on $u_0$. Invoking now the definition [Eq. (48)] of the classical turning point $u_0$ and $K_0(u) \simeq \sqrt{\pi/2u} e^{-u}$, we find that

$$\xi(R') \simeq \sqrt{\frac{6}{(\kappa\ell)^2}} |E|^{1/2} \left( U - u_0 + \frac{1}{2} \right). \tag{54}$$

In the asymptotic limit of large cell size the condition $U > u_0 > 1$ is satisfied and one can obtain the following approximate expression:

$$|E| \simeq \frac{(\kappa\ell)^2 \xi^2}{6(U-u_0)^2 + \frac{1}{2}} \simeq \frac{(\xi\ell)^2}{6R'^2}. \tag{55}$$

Here we need to keep in mind that $\xi$ is a function only of $M_0$ and is always within the interval $3\pi/4 < \xi(R') < 5\pi/6$. Since this solution is only valid for large enough $R'$ [the opposite limit is covered by Eq. (46)] the above equation effectively claims that

$$-\frac{3(\pi\ell)^2}{32R'^2} \lesssim E \lesssim -\frac{25(\pi\ell)^2}{216R'^2}. \tag{56}$$

We see that the free energy has a long-range attractive tail, as already tentatively derived in the reciprocal space calculations of Eq. (30), falling off algebraically with the size of the Wigner–Seitz cell. The form of the dependence of the complete WKB solution on $R'$ (see Fig. 7) completely corroborates the derived asymptotic forms. Since the radius of the WS cell is derived from the (2D) density of the macroions, $\rho_M = 1/\pi R'^2$, we can immediately write down that

$$E \simeq -\gamma(\ell^2 \rho_M),$$

where

$$0.094\pi^3 < \gamma < 0.116\pi^3. \tag{57}$$

It is surprising that such a good estimate can be obtained for the magnitude of the polyelectrolyte bridging interaction in the system under investigation. We are not aware of any simple scaling argument that would reproduce the exponent of 1 in the density dependence of the bridging attraction. One of course has to be aware that this is a limiting form valid

only within restrictive conditions and constraints detailed above.

## VI. RESULTS AND CONCLUSIONS

This work analyzes the polyelectrolyte-mediated interactions in an array of oppositely charged macroions. Apart from geometry and dimensionality this is the same problem as already discussed for the case of two charged surfaces with intervening polyelectrolyte chains.[11] The physics in both cases is the same but the nature of the two-dimensional array makes the range of the polyelectrolyte-mediated interactions much larger.

In our analysis of the polymer-mediated interactions on a 2D lattice of macroions we start from two different directions yielding similar results:

- We formulate the polyelectrolyte on a 2D lattice problem that we were able to solve by applying the methods developed to describe electrons in an ionic crystalline lattice. The only fundamental difference is that in the polyelectrolyte case the lattice-polymer interaction potential is of a screened Debye–Hückel form as opposed to the unscreened Coulomb form appropriate for electrons in a crystal. We derive that for sufficiently strong polyelectrolyte-macroion electrostatic coupling the free energy exhibits attractive, i.e., bridging interactions, falling off approximately linearly with the macroion density but with relatively poorly defined absolute magnitude.
- We formulate the polyelectrolyte-mediated interactions in the framework of a Wigner–Seitz model, where a single cell with appropriate boundary conditions is substituted for the whole lattice. This calculation lent final support for the rather tentative conclusions of the first calculation. We again derive bridging interactions at sufficiently large polyelectrolyte-macroion electrostatic coupling and obtain an exact limiting law for small macroion densities, of the form suggested by the lattice calculation, but in addition we are able to derive also a well-defined numerically bracketed coefficient.

By analyzing the energy eigenvalue equation in the lattice approach for different RLV basis sets we were able to guess that the lowest-lying eigenenergy has a long-range tail in the limit of small macroion densities. In fact, the only case that we were able to solve analytically suggested that in the asymptotic limit of vanishing macroion density, i.e., $R\to\infty$, the polyelectrolyte free energy behaves as $\mathcal{F}\sim R^{-2}$. But since this result gives only one part of the total eigenenergy dependence on macroion density, it is by itself of rather limited validity. Fortunately we were able to corroborate these tentative results by a more detailed WS calculation. The same reasoning applies also for the tentative identification of a branching point in the solution that delimits a regime where polyelectrolyte-mediated interactions are repulsive, corresponding to steric compression of the polyelectrolyte chains by the macroions, from the one where they turn attractive, corresponding to bridging configurations of the polyelectrolyte chain between the macroions.

The Wigner–Seitz model itself does not lead to any simple analytical estimates since the Schrödinger equation is not solvable by simple quadratures. We thus went one step further and applied the WKB approximation to obtain simple closed form solutions of the Schrödinger equation. The WKB solution yielded simple analytical forms of the asymptotic behavior of the polyelectrolyte free energy. We again were able to prove that indeed in the asymptotic limit of small macroion density, the polyelectrolyte free energy behaves as $\mathcal{F}\sim R^{-2}$, and we obtained a good estimate for the numerical coefficient in this scaling relationship. We established directly that there is a critical value of the strength of the polyelectrolyte-macroion interaction $w_c$ that separates the bridging from the compression regime and thus attractions from repulsions. This appears to be a salient feature of the behavior of this system. We are thus confident that even more detailed numerical solutions of this problem will show similar bifurcation in the nature of polyelectrolyte-mediated interaction.

Similar features of the polyelectrolyte-mediated interaction are clearly seen also in experiments on DNA-polycation complexes.[16] The polycations, being poly-L-lysine and poly-L-arginine, are both about 30–100 units long and sufficiently flexible and charged to be well described by the Edwards model. Thus our calculation may provide an alternative interpretation to these experimental findings that does not rely on strong-coupling electrostatics.[16] Our results also show that for large macroion densities the polyelectrolytes are sterically confined and localized in the interstices of the 2D lattice. Here a strong-coupling electrostatics analysis[16] might be a much better choice since our model describes a spatially inherently disordered polymer. On the other hand for small macroion densities, where polyelectrolyte chains could be well described as disordered, our approach might carry more weight than strong-coupling electrostatics that relies mostly on ordered configurations of the polyelectrolyte chains. It may well be, however, that both effects, strong-coupling electrostatics as well as polyelectrolyte bridging, combine to give the complex salt-dependent interactions seen in this experiment.

In spite of the similarity between the 1D (Ref. 11) and 2D case of polyelectrolyte bridging interactions, there is a huge difference in the asymptotic form of the polyelectrolyte free energy. In 1D the free energy decays exponentially with the separation between the two charged surfaces, where the characteristic exponent is on the order of the single polymer link size.[11] In 2D, however, the free energy decays algebraically with the macroion lattice spacing and is thus of long range. The difference is basically due to the different topologies of the 1D and 2D cases. In the 1D case a single long polyelectrolyte chain can only bridge two surfaces. Even when there is an array of surfaces the polyelectrolyte chains cannot bridge next neighbors nor, even less, surfaces that are further apart. In the 2D case a single very long chain can bridge the spacing between many different macroions and can thus confer a much stronger bridging interaction to the whole assembly. This many-body multiplication of bridging also extends the range of the interactions, turning short-range bridging into long-range bridging.

One should note at the end that Edwards model on which our calculation is based, describes inherently flexible polymer chains. For semiflexible stiff chains the description would by necessity have to start from a wormlike chain model. Unfortunately this model is much more difficult to solve in the presence of external interaction fields such as screened Coulomb electrostatics.[25]

In this work we were mostly concerned with the conceptual and formal issues of how to calculate polyelectrolyte bridging interaction in the 2D macromolecular arrays. We do not aim for extensive numerical computations and possible comparison with the phase behavior of this system in relevant experiments.[16] In that case one would have to add the polyelectrolyte-mediated interaction terms $\mathcal{F}$ of Eq. (11) to direct macroion–macroion interactions described by the free energy $\mathcal{F}_M$ that have been resolved and understood on a molecular level for the case of DNA.[26] Such an investigation would thus focus on the behavior of the total free energy of the array, as a function the macroion density $\rho_M$. We will embark on this study in a forthcoming publication.

## ACKNOWLEDGMENTS

We would like to thank Per Lyngs Hansen for numerous discussions regarding polyelectrolytes and their theoretical description. We would also like to thank J. DeRouchey, R. Netz, and J. Rädler for sending us their work prior to publication. One of the authors (W.M.S.) would also like to acknowledge the support of the Department of Energy, under Grant No. DE-FG03-96ER45598. Another author (R.P.) would like to acknowledge the support of the Ministry of Education, Science and Sport of Slovenia under Grant No. P1-0055.

[1]F. Oosawa, *Polyelectrolyes* (Marcel Dekker, New York, 1971).
[2]J.-L. Barrat and J.-F. Joanny, Adv. Chem. Phys. **94**, 1 (1996).
[3]M. Rubinshtein and R. H. Colby, *Polymer Physics* (Oxford University Press, Oxford, 2003).
[4]D. Napper, *Polymeric Stabilisation of Colloidal Dispersions* (Academic, New York, 1983).
[5]D. Boal, *Mechanics of the Cell* (Cambridge University Press, Cambridge, 2002).
[6]For a good introduction, see *Electrostatic Effects in Soft Matter and Biophysics*, edited by C. Holm, P. Kekicheff, and R. Podgornik (Kluwer Academic, New York, 2001).
[7]R. Podgornik, J. Polym. Sci., Part B: Polym. Phys. **42**, 3539 (2004).
[8]R. R. Netz and D. Andelman, Phys. Rep. **380**, 1 (2003).
[9]E. Eisenriegler, *Polymers Near Surfaces: Conformation Properties and Relation to Critical Phenomena* (World Scientific, Singapore, 1993); M. A. Cohen Stuart, G. J. Fleer, and J. M. H. M. Scheutjens, *Polymers at Interfaces* (Chapman and Hall, London, 1993).
[10]M. Muthukumar, J. Chem. Phys. **86**, 7230 (1987).
[11]R. Podgornik, J. Phys. Chem. **95**, 5249 (1991); R. Podgornik, J. Phys. Chem. **96**, 884 (1992).
[12]I. Borukhov, D. Andelman, and H. Orland, J. Phys. Chem. **103**, 5042 (1999).
[13]X. Châtellier and J.-F. Joanny, J Phys II France **6**, 1669 (1996).
[14]R. Podgornik and B. Jönsson, Europhys. Lett. **24**, 501 (1993); R. Podgornik, T. Åkesson, and B. Jönsson, J. Chem. Phys. **102**, 9423 (1995).
[15]R. Podgornik, J. Chem. Phys. **118**, 11286 (2003).
[16]J. DeRouchey, R. R. Netz, and J. O. Rädler, Eur. Phys. J. E **16**, 17 (2005).
[17]M. Doi and S. F. Edwards, *The Theory of Polymer Dynamics* (Clarendon, Oxford, 1986).
[18]R. Podgornik, J. Chem. Phys. **91**, 5840 (1989).
[19]D. F. Evans and H. Wennerstrm, *The Colloidal Domain: Where Physics, Chemistry, Biology, and Technology Meet*, (Wiley, New York, 1999).
[20]V. Lorman, R. Podgornik, and B. Žekš, Phys. Rev. Lett. **87**, 218101-4 (2001).
[21]K. F. Freed, *Renormalization Group Theory of Macromolecules* (Wiley, New York, 1987).
[22]N. W. Ashcroft and N. D. Mermin, *Solid State Physics*, 1st ed. (Saunders College Publishing, New York, 1976).
[23]P.-G. de Gennes, *Scaling Concepts in Polymer Physics* (Cornell University Press, New York, 1979).
[24]A. B. Migdal and A. J. Leggett, edited by W. A. Benjamin *Qualitative Methods in Quantum Theory* (Perseus, Reading, Massachusetts, 2000).
[25]P. L. Hansen and R. Podgornik, J. Chem. Phys. **114**, 8637 (2001).
[26]R. Podgornik, D. C. Rau, and V. A. Parsegian, Macromolecules **22**, 1780 (1989); R. Podgornik, D. C. Rau, and V. A. Parsegian, Biophys. J. **66**, 962 (1994).